Universiteit
Leiden
The Netherlands

Magnetism and magnetization dynamics in thin film ferromagnets

Verhagen, T.G.A.

Citation

Verhagen, T. G. A. (2014, February 26). *Magnetism and magnetization dynamics in thin film ferromagnets*. *Casimir PhD Series*. Retrieved from https://hdl.handle.net/1887/24306

Version:	Not Applicable (or Unknown)
License:	Leiden University Non-exclusive license
Downloaded from:	https://hdl.handle.net/1887/24306

Note: To cite this publication please use the final published version (if applicable).

Cover Page

Universiteit Leiden

The handle http://hdl.handle.net/1887/24306 holds various files of this Leiden University dissertation

Author: Verhagen, T.G.A.
Title: Magnetism and magnetization dynamics in thin film ferromagnets
Issue Date: 2014-02-26

CHAPTER 3

Point contact spectroscopy[1]

3.1 Point contact spectroscopy - theoretical

The electrical resistance of a contact with a size smaller than the electronic mean free path is only determined by the number of quantum channels and their transmission probability through this contact. These contacts, called Sharvin or point contacts (PC), were first used to determine the electron-phonon spectral function in normal metals.

Due to the size of the constriction, from a few nanometers up to hundreds of nanometers, it is possible to create very high current densities (of the order of 10^{10} A/m^2) without excessive heating effects. This allows to observe physical effects that cannot be seen with lower current densities like the spin-transfer torque.

The point contact geometry is also the preferred geometry to study the spin-flip laser, because the very high current density needed to obtain a non-equilibrium inverse population of the two spin-split levels. Furthermore, the point contact spectroscopy technique can be used to obtain information about the relaxation processes at the interface of the ferromagnet/normal metal.

The transport through such point contacts can be characterized by different transport regimes, depending on how the diameter d of the

[1] Parts of this chapter have been published in: E. Tartaglini, T.G.A. Verhagen, F. Galli, M.L. Trouwborst, R. Müller, T. Shiota, J. Aarts and J.M. van Ruitenbeek, *New directions in point-contact spectroscopy based on scanning tunneling microscopy techniques*, Fizika Nizkikh Temperatur **39** 249-260 (2013).

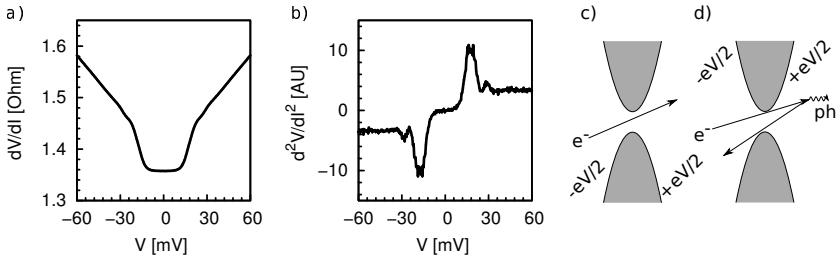

Figure 3.1: The in-house measured V - dV/dI and the numerically calculated V - d^2V/dI^2 characteristics for a Cu-Cu point contact are plotted in a) and b) respectively. Due to the electron-phonon interaction, an increase in resistance can be observed around 16, 19 and 26 eV appearing as peaks in the d^2V/dI^2. Electrons travelling through a constriction gain an excess energy eV c). The electron-phonon interaction in a ballistic point contact can result in a backscatter event, d).

point contact scales to the elastic ℓ_{el} and inelastic ℓ_{in} electron mean free path and the Fermi wavelength λ_{F} of electrons. We can then distinguish the thermal regime, where $d \gg \ell_{\text{el}}$, ℓ_{in}, λ_{F}, the diffusive regime $\sqrt{\ell_{\text{el}}\ell_{\text{in}}} \gg d \gg \ell_{\text{el}}$, λ_{F}, the ballistic regime ℓ_{el}, $\ell_{\text{in}} \gg d \gg \lambda_{\text{F}}$ and the quantum regime, where ℓ_{el}, ℓ_{in}, $\lambda_{\text{F}} \gg$ d.

Below, we show and discuss a number of PC measurements which were meant as a first step to the final observation of radiation coming from the point contact. Inversely, it was attempted to observe spin flip processes due to irradiation, using a normal metal tip on a ferromagnetic film.

3.1.1 Electrical transport in a point contact

In 1965, Sharvin showed that the resistance of a ballistic point contact between two normal metals only depends on the diameter d of the point contact. The Sharvin resistance [76] is equal to

$$R_{\text{Sh}} = \frac{16\rho\ell_{\text{el}}}{3\pi d^2}, \tag{3.1}$$

where ρ is the resistivity of the material.

In Figure 3.1.a, the measured differential conductance dV/dI as a function of the applied voltage V and in Figure 3.1.b the numerically calculated $\text{d}^2\text{V}/\text{dI}^2$ as a function of the applied voltage V are shown of a Cu-Cu point contact. A clear non-linearity can be observed that

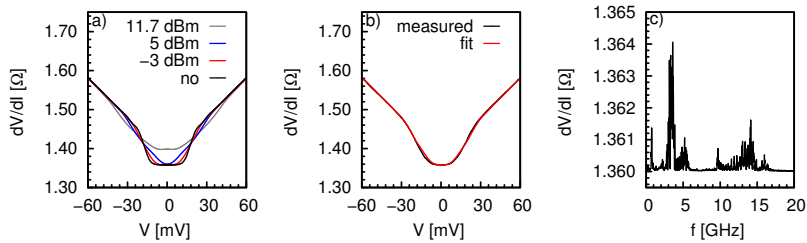

Figure 3.2: a) The resistance of a Cu-Cu point contact when it is irradiated with 4 GHz radiation at different power levels. In b), the influence of the radiation is modelled, assuming that the point contact works as a classical rectifier. c) shows the frequency dependence of the resistance of a point contact when it is biased at 15 mV.

can be attributed to electron-phonon scattering processes. As shown in Figure 3.1.c, for low applied biases, electrons passing through the constriction gain an excess energy eV. The electron can relax via an inelastic scattering event with a phonon. When this scattering takes place close to the constriction, the electron can be scattered back through the constriction (Figure 3.1.d) causing a backflow current.

The backflow current can be calculated, by assuming an energy dependent scattering length, $l(eV) = v_F \tau_{\text{e-ph}}(eV)$, with v_F the Fermi velocity and $\tau_{\text{e-ph}}$ the energy dependent electron-phonon scattering time

$$\frac{1}{\tau_{\text{e-ph}}(eV)} = \frac{2\pi}{\hbar} \int_0^{eV} \alpha^2(\epsilon) F(\epsilon) d\epsilon, \tag{3.2}$$

with $\alpha^2(\epsilon)F(\epsilon)$, the electron-phonon interaction function. It follows straightforwardly that $\mathrm{d^2V/dI^2}$ is then equal to

$$\frac{dR}{dV} \propto \frac{d^2V}{dI^2} \tag{3.3}$$

$$\propto R_{\text{Sh}} \frac{3\pi^2 ed}{8\hbar v_F} \alpha^2(eV) F(eV). \tag{3.4}$$

So, by measuring the V - d^2V/dI^2 of a ballistic point-contact, the electron-phonon interaction can be obtained.

Point contact spectroscopy (PCS) has developed into an ideal tool to probe a whole range of elementary excitations in all kinds of systems. In recent years, PCS became an important tool to probe the order parameter in superconducting materials like the cuprates [77] and

the pnictides [78], to measure the spin polarization of magnetic materials [79] and to measure transport properties of single atoms and molecules where the local vibration modes of the atoms or molecules can be detected [80]. Also, PCS helped to better understand the STT effect [35, 81]. The ability of PCS to distinguish between backscattering and impurity scattering clarified the role of impurities by the single-interface STT [81].

3.1.2 Irradiating point contacts

When irradiating a point contact with radiation with frequency ν, the tip works as an effective antenna and the applied radiation induces oscillatory potentials $V(t) = V_0 + V_{\text{ac}} \cos(2\pi\nu t)$ across the point contact. The response to the irradiation can be described as a classical detector where the induced oscillating potentials combine via a non-linearity into an ac-rectification, if the energy of the photons is smaller than the width of the non-linearity [82]. In Figure 3.2.a, the influence of irradiating a Cu-Cu point contact with 4 GHz radiation is shown. The current-voltage characteristic $I(V)$ of an irradiated point contact can be modelled as

$$I(V) = \frac{1}{2\nu} \int_0^{1/2\nu} I_0(V_0 + V_{\text{ac}} \cos(2\pi\nu t))dt, \tag{3.5}$$

where $I_0(V_0)$ is the current-voltage characteristic in the absence of microwave radiation. In Figure 3.2.b, equation 3.5 is fitted to the 2 dBm curve of the measured spectra from Figure 3.2.a with a V_{ac} of 8 mV. If a constant bias voltage is applied to the point contact so that it is tuned to the non-linear part of the characteristic, the point contact will detect radiation by the amplitude of the rectified signal. In Figure 3.2.c, the frequency dependence of the signal detected by a point contact with a constant bias is shown. It shows that the coupling-efficiency of the point contact is strongly frequency dependent.

3.2 Point contact spectroscopy - experimental

In 1974 Yanson [83] used a metal-insulator-metal tunnel junction having a short, to measure energy resolved spectroscopy of the electronic scattering inside the metal, and could directly measure the energy dependence of the electron-phonon interaction. The introduction of the needle-anvil method by Jansen et al. [84] in 1976 was a further improvement. With this technique a sharply etched metal wire, the needle, was

pressed using a micrometer screw into a flat metal surface, the anvil, to form a point contact. The contact size can be adjusted by fine-tuning the pressure applied to the tip with the micrometer screw. Transport in such point contacts is ballistic since contacts diameters are usually much smaller than the electron mean free path.

In the last 20 years also the development of STM, at or below liquid helium temperatures improved enormously [85]. One of the biggest problems in the design of low temperature STMs was the piezoelectric positioning system that often fails to work at these temperatures. The Beetle [86, 87] and the Pan-type [88] walker coarse positioner solved this problem and are now widely used in low temperature STMs. Nowadays, one can even buy commercial piezo positioners that reliably operate at low temperatures and at high magnetic fields [89].

3.2.1 Point contact spectroscopy measurement

In a non-UHV environment, very thin native oxide layers, plus adsorbates of organic materials, are always present on both the tip and sample. A very important requirement is to make a clean metallic contact between the sample and the tip. For this purpose the tip is moved slowly with a micrometer screw or a piezo positioner to the sample, and when both parts are firmly pressed together, the greatest stress occurs at the point where the needle touches the sample. Here, the oxide layer breaks and forms a small direct metallic contact between the two parts: the point contact. Note that the presence of the oxide layer is not only a disadvantage: it can be helpful because it reduces the conducting electrical contact area between the tip and sample, while the mechanical contact area is much larger so that stable contact sizes between 4 and 100 nm can be made.

3.2.1.1 Tip and sample preparation

For various types of PCS experiments, different tip materials were used. We used Cu wires with a diameter of 125 and 500 μm, Pb wires with a diameter of 500 μm and Nb wires with a diameter of 250 μm during the experiments. Although thick wires can produce good PCS spectra, the stiffness of the wire tends to damage the sample within a few cycles of breaking and making contacts. Using thinner wires and adding an extra loop with a diameter of approximately 2 mm into the wire, the force the tip can exert on the sample is reduced and the number of contacts that can be made and broken is increased.

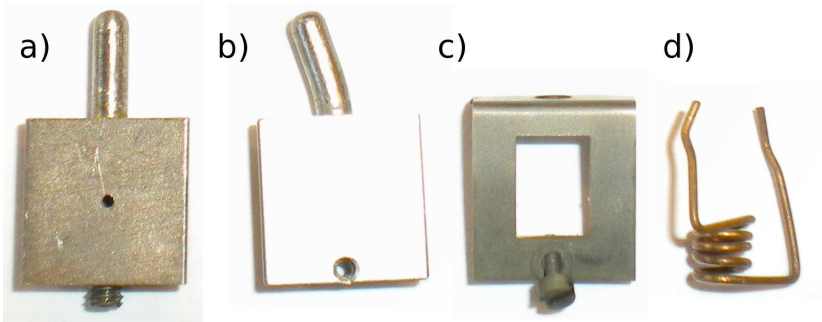

Figure 3.3: a) 9×9 mm^2 tip holder with on the bottom side the screw for tighting the mount of the tip wire. b) 9×9 mm^2 sampleholder onto which the substrate with the thin film or foil is glued. The hole in front of the sample holder is used to mount the Ti cap (c). For insulating substrates, a Ti cap (c) or Cu spring (d) are used to for making an electrical contact with the sampleholder.

In Figure 3.3.a, the titanium tip holder is shown were the tip is mounted in the hole and anchored with a titanium screw. After mounting the tip, the tip was etched to remove the thick native oxide layer. Cu tips were etched in a droplet of nitric acid, which resulted in a removal of the native oxide layer, which results i a rather flat apex. To obtain a conical apex, tips were electrochemically etched in a 25% HCl solution [90]. After etching, the tip has a typical conical apex of 10 μm as can be seen in Figure 3.4 for a Cu tip.

Samples we used were either a thin film grown using sputter deposition or a thin sheet or foil. In Figure 3.3.c, the Ti sample holder is shown onto which the substrate or foil can be glued using silver paint. To make electrical contact to thin films grown on insulating substrates, the edges of the film were connected to the sample holder by means of a titanium cap (see Figure 3.3.b) or a copper spring (see Figure 3.3.d) to the sample holder.

Grown thin films were glued as quickly as possible onto the sample holder after the samples were removed from the deposition system to prevent the formation of a thick oxide layer. Foils and sheets were first glued onto the sample holder, whereafter the native oxide layer present on them was etched away using a nitric acid or 25% HCl solution until the surface looked shiny.

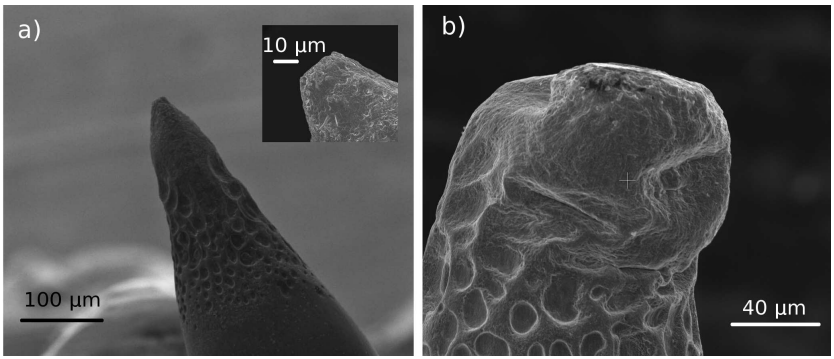

Figure 3.4: A scanning electron microscopy image of two different electrochemically etched Cu-tips before (a) and after (b) a point contact spectroscopy measurement with a piezo positioner.

3.2.1.2 Measurements

The point contact measurements were performed at 4.2 K in a liquid helium storage vessel, bath cryostat or in an optical cryostat with a variable temperature insert. The conductance and the phonon spectrum were measured using a current biased lock-in technique.

The point contact was made by carefully moving the tip with the piezo positioner or micrometer screw while simultaneously measuring the resistance between the tip and the sample. Before the contact was formed, a high constant resistance was observed, which is the result of combination of the native oxide and the vacuum gap between the tip and sample. When making the contact, the tip will first approach the oxide covered surface layer of the sample. When the tip touches the sample, it needs also to break the thin oxide layer to form a metallic contact. Unfortunately, we cannot distinguish these processes during the approach.

3.2.2 Scanning point contact spectroscopy

The measurements with the traditional micrometer-controlled needle anvil technique are often limited to a single position on the sample due to a lack of the ability to move the sample in a controllable way. A big improvement in PCS would be the ability to map the PCS data on the surface by such controlled motion of the sample. In Leiden, we started to explore the possibility to do scanning PCS. For this purpose, Simon

Kelly built a scanning PCS system, where he used a modified STM-insert [91] with an Attocube ANPz101 z-direction nanopositioner and a scantube to move the tip in the x- and y-direction, which is shown in Figure 3.5. For the first tests, only the z-direction was used.

We noticed that if we made our first contacts with a fresh tip and fresh sample, when we made a metallic contact and retracted the tip just far enough that we lose the metallic contact, the next approach takes much longer than expected from the retraction distance. The crack in the oxide layer forms at a different place than before and the piezo positioner needs a lot of steps to break the oxide layer. It is also possible that instead of breaking the oxide layer, a metallic contact is formed by deforming the tip, as can be seen in Figure 3.4.b, where the tip is imaged just after good ballistic contacts were measured.

The main drawback of the low-temperature piezo positioners is that they are designed for accurate positioning (several tens of a nm), but not to apply forces large enough to break oxide layers. In contrast, the micrometer screw can continuously apply the same force and break the oxide layer in a continuous way.

3.2.3 Micrometer screw point contact spectroscopy

To circumvent the problem of piezo positioners, also PCS inserts were built where the tip was connected via a drive shaft to a micrometer screw mechanism, which is capable of moving the tip with 1 μm per revolution. This established method [92] results in a reliable way of making point contacts. In Figure 3.6, two PCS inserts that were built are shown. The insert in Figure 3.6.a is designed such that it fits in the variable temperature insert of an Oxford optical cryostat without blocking the optical path too much. Figure 3.6.b shows the vertical PCS insert for a bath cryostat with a solenoid superconducting magnet. By placing the sample- and tipholder vertically, the magnetic field is in-plane.

3.3 Spin-flip laser

One possible experimental realization to test the theoretical prediction of a metal based spin-flip laser as described in Section 2.5 is shown in Figure 3.7.a. Using the mechanical point contact geometry, an F/N contact is created. As the ferromagnet a thin $SmCo_5$ film is used, which has the advantage that it has a large coercive field which results in a wide magnetic field and frequency domain to test the theory. In the

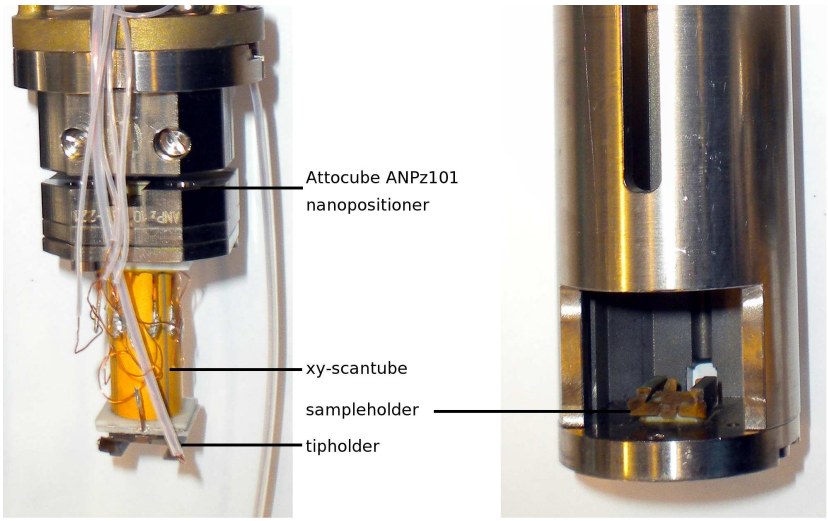

Figure 3.5: Point contact spectroscopy head based on the Attocube ANPz101 nanopositioner and a scan tube to scan in the x- and y-direction. The tipholder is mounted below the scan tube and the sample holder is mounted at the bottom of the protection cap, that is mounted around the piezo nanopositioners.

literature, many groups have shown that thin Sm-Co films with a large coercive field can be grown using sputter deposition [93–99]. The advantage of thin films is that different materials as a capping layers can be used, to protect the Sm-Co surface or to manipulate the properties of the spin-flip laser. As the normal metal part of the spin-flip laser, a Cu tip is used.

It is very difficult to detect the emission of a few photons that might be emitted from the F/N point contact. We therefore irradiate the point contact with microwave radiation, as is shown in the configuration of Figure 2.7.c and detect spectroscopically if spin-flip processes are happening. With a constant voltage bias, the resistance of the irradiated point contact is measured as a function of the applied magnetic field. When the resonance condition, equation 2.21, is fulfilled, a peak in the resistance as illustrated in Figure 3.7.b is expected. There must be a linear relation between the resonance field and the applied microwave radiation, as shown in Figure 3.7.c.

In Figure 3.8.a, typical PCS measurements are shown that were done

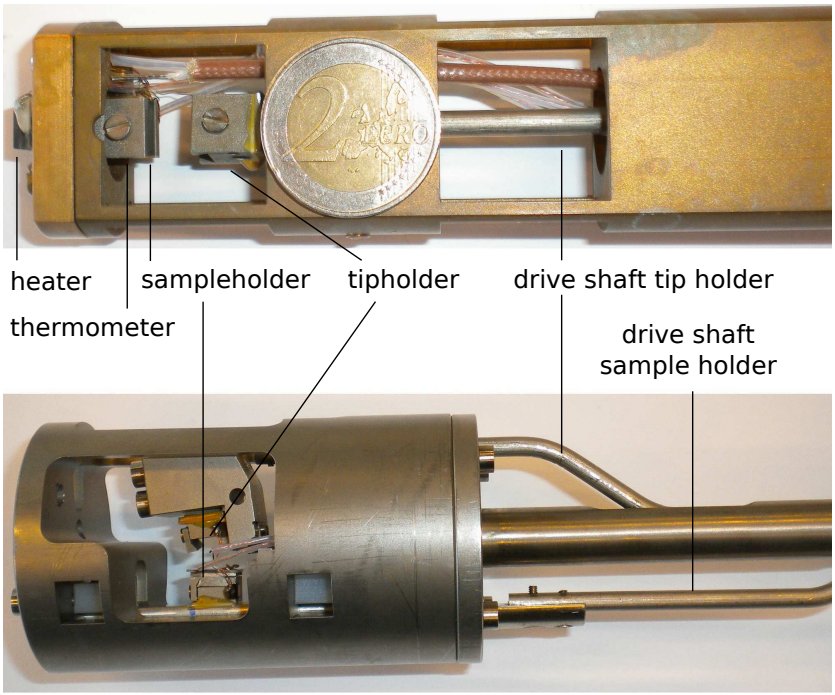

Figure 3.6: a) Micrometer screw based point contact spectroscopy insert. The sample- and tipholder can be mounted and secured with a screw. The tipholder is attached to a drive shaft, that is connected to a micrometer screw, which stays at room temperature (not shown). The temperature is measured using a thermometer that can be mounted just below the sample- or tipholder and at the bottom of the insert a heater is mounted to control the temperature. Also an open-ended coax cable is present to irradiate the sample. b) Micrometer screw based vertical point contact spectroscopy insert, that is also able to move the sample using another micrometer screw.

in Leiden on Sm-Co thin films deposited by sputtering (see Chapter 4) with a Cu capping layer. None of the measurements on the Sm-Co films has shown a signature of the spin-transfer-torque (STT) peaks or the Zeeman-resonances. However, measurements done at the B. Verkin Institute for Low Temperature Physics and Engineering of the National Academy of Sciences of Ukraine (ILT), showed for several films the STT effect, as shown in Figure 3.8.b and even an indication of the spin-flip laser effect, as shown in Figure 3.8.c. Unfortunately, also at ILT only a few of these measurements were successful and no studies could be done of the resonance field versus microwave frequency or the influence of the applied bias.

3.4 Discussion

Basically, there are two ingredients that might be responsible for the low reproducibility of the experiments. First, the surface quality of the Sm-Co is not well defined. From the growth of the Sm-Co thin films on MgO(100) and MgO(110) substrates, we learned that these films are generally not single crystalline. Furthermore, in Chapter 4 we show how different the crystallites can behave with small variations in the Sm-Co composition and the sputter gas pressure.

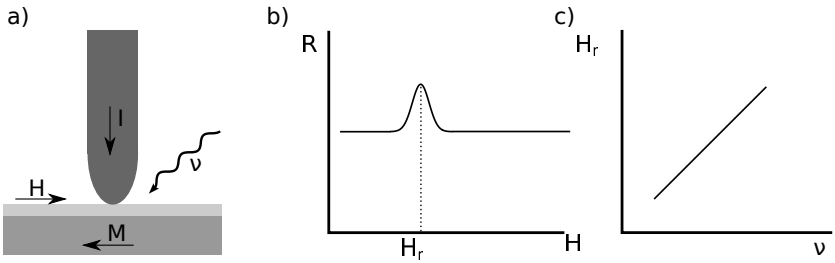

Figure 3.7: a) Experimental set-up for measuring the spin-flip laser using a mechanical point contact. b) The expected dependence of the resistance R of the point contact as a function of the applied magnetic field B for a point contact with a constant bias. When irradiating the point contact with microwave radiation with a frequency ν, there is a increase in resistance when the resonance condition, equation 2.21, is fulfilled. c) The resonance magnetic field as a function of the irradiating frequency is expected to show a linear relation for the Zeeman-splitting based spin-flip laser.

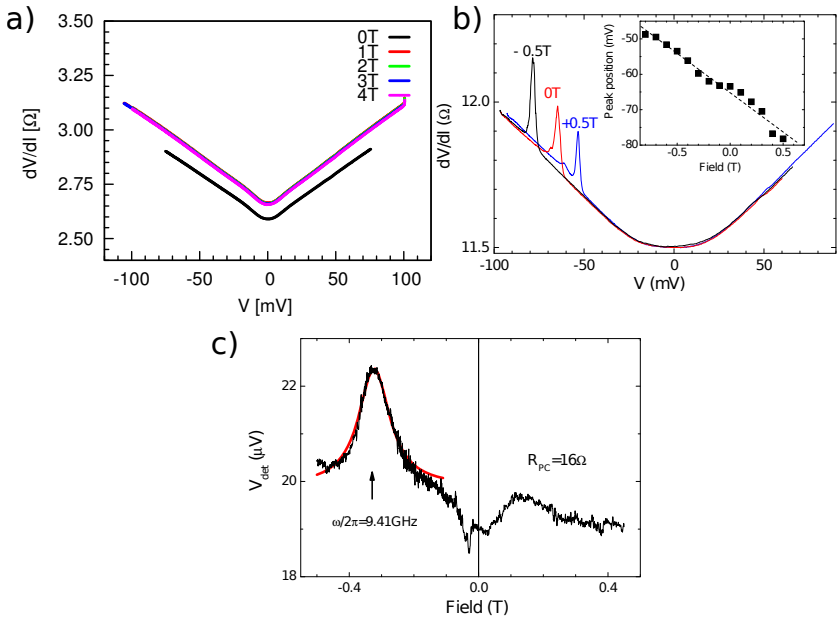

Figure 3.8: a) Typical Leiden point contacts measurements on a SmCo/Cu thin film with a Cu tip, with and without an applied in-plane magnetic field. The 1, 2, 3 and 4 T curves are overlaying each other. b) The differential resistance of a $SmCo_5$/Cu point contact measured at the B. Verkin Institute for Low Temperature Physics and Engineering of the National Academy of Sciences of Ukraine as a function of the bias voltage at an applied field of -1.0, 0 and 0.5 T. A clear STT peak is visible. In the inset, the position of the STT peak versus the magnetic field is plotted. c) Detected voltage V_{det} as a function of the applied magnetic field for a $SmCo_5$/Cu point contact under microwave irradiation at 4.2 K and biased with -20 mV. The arrow indicates the resonant magnetic field H_r for which the photon energy fulfills the resonance condition. Figure b) and c) taken from [74]

At ILT, $SmCo_5$ films capped with 3-5 nm thick Cu, Cr, Al, Fe or Co layers were investigated, that were grown at the Leibniz Institute for Solid State and Materials Research in Dresden. PCS on $SmCo_5$ films with a Cr capping layer and Cu or Ag tips showed non-metallic behaviour, likely due to forming of a dielectric layer on the surface (probably chromium oxide), which is good for protecting the ferromagnetic surface but makes it difficult to form stable metallic tip-surface point contacts. $SmCo_5$ films with an Al, Fe and Co capping layer showed metallic behaviour, but ILT did not not succeed to observe resistance features associated with resonant photon emission or absorption [100]. Films capped with a thin Cu layer resulted in the observation of the expected features. In Figure 3.8.b, the observed STT is shown for different applied magnetic fields. The observation of the STT tells, that the $SmCo_5$/Cu interface is spin polarized. Multiple measurements on the $SmCo_5$/Cu samples showed the degradation of the surface properties, which potentially has been the cause for poor reproducibility of the results.

The other ingredient where we have little control over is the exact orientation of the magnetization direction in the $SmCo_5$ domain in the point contact and the direction of the magnetic field component of the applied microwave radiation.

Although in some of the point contacts the STT effect is observed, the orientation of the magnetization in the $SmCo_5$ domain where the Cu tip is touching is unknown. When the contact with the Cu tip is made, some pressure is applied to the $SmCo_5$ film. The pressure to the film can induce locally stress to the film, which can rotate the in-plane magnetization into a slightly different direction. This is supported by the observation of the STT, which needs a non-collinear magnetization to convert a spin current to a torque.

3.5 Outlook

To obtain more control over the formation of the point contacts, lithographic point contacts can be used instead of the point contacts that were made using the traditional needle-anvil method. When growing the different layers in-situ, there is a clean interface between the different materials. Furthermore, no extra stress to the contact with the needle is induced in the Sm-Co film which might change the (magnetic) properties of the Sm-Co.

We also sought for a different way to characterize the F_1/N, $F_1/N/F_2$ and $F_1/f/F_2$ configurations with respect to the behaviour of spin. In

particular, it would be useful to know whether spin can be transferred to and from the Sm-Co layer. We therefore initiated a set of experiments in which ferromagnetic resonance (FMR) is used to pump spin out of an F layer and study which properties play a crucial role in the spin torque and spin pumping phenomena. Co films were used for these measurements (see Chapters 5 and 6).

Furthermore, the combination of a lithographic point contact with the spin Hall effect might be an interesting route to create a spin-flip laser. The spin Hall effect makes it possible to inject a fully polarized spin current into an adjacent layer, which helps to circumvent the usage of traditional ferromagnets that possesses low coercive fields or hard ferromagnets that are complicate to grow (see Chapter 4).